第33卷第11期　　焊　接　学　报　　Vol. 33　No. 11
2012年11月　　TRANSACTIONS OF THE CHINA WELDING INSTITUTION　　November　2012

多次焊补对高速列车铝合金焊接接头的影响

于金朋[1,2]， 张立民[1]， 张卫华[1]， 陈　辉[1]， 马纪军[2]

(1. 西南交通大学 牵引动力国家重点实验室，成都　610031; 2. 唐山轨道客车有限责任有限公司，丰润　063035)

于金朋

摘　要: 文中对EN 5083 铝合金对接接头进行了一次、二次和三次焊补等试验. 进行了微观组织、硬度、拉伸、冲击、抗剪强度和压入率的分析. 结果表明，焊补层的晶粒比原焊缝的大，α(Al) +β(Mg_2Al_3)共晶网状组织变得更大. 焊补层熔合区的受热析出的第二相也更多. 三次焊补之间的硬度、抗拉强度、冲击韧性变化不大，断口剪切唇区很明显，说明都是韧性断裂. 焊缝处抗剪强度比较低. 焊补后，抗剪切能力下降，但是趋于稳定，三次焊补的质量几乎和二次焊补一样，说明在控制好工艺和减少焊接缺陷的情况下，试件有进行三次焊补的可能.

关键词: EN 5083 铝合金; 多次焊补; 第二相; 韧性断裂

中图分类号: G405　　**文献标识码**: A　　**文章编号**: 0253-360X(2012)11-0077-06

0　序　　言

铝合金已普遍应用于轨道车辆的制造当中[1,2]. 铝合金焊接过程中常出现焊接工艺所不允许的焊接缺陷如裂纹、夹杂、气孔、未焊透等，而造成焊缝的返修补焊[3]. 为了节约原材料成本和制造成本，在满足车辆设计要求的条件下有必要对产生焊接缺陷的焊接接头进行焊补. 文献[4]研究认为，补焊区的非均匀加热较为严重，且存在一定程度的成份偏析和结构应力，从而导致补焊区的力学性能与未焊补层存在差别，影响焊补层的有效使用.

按照德国标准EN15085《轨道车辆及其部件的焊接》铝合金焊接技术条件的要求，只能进行两次补焊，从一定程度上造成了材料的浪费. 课题组针对高速列车铝合金焊接接头进行了大量的失效分析，针对某类型高速列车用EN AW-5083铝合金为研究对象，设计提出三次焊补的方法，研究焊补对焊接接头的微观组织结构和力学性能的影响，评估焊接接头的多次焊补的可行性.

1　试验方法

试验选用EN AW-5083铝合金板材为母材，试件的几何尺寸为500 mm×100 mm×10 mm，选取ER5356铝镁合金焊丝，焊丝直径为ϕ2.0 mm. EN AW-5083铝合金母材和ER5356焊丝的化学成分见表1所示.

表1　母材及焊丝的化学成分(质量分数，%)

Table 1　Chemical compositions of matrix and welding wire

	Zn	Mg	Cu	Mn	Ti	Si	Fe	Al
母材	0.25	4.0~4.9	0.1	0.4~1.0	0.15	0.4	0.4	余量
焊丝	0.1	4.5~5.5	0.1	0.05~0.20	0.06~0.20	0.25	0.4	余量

采用双脉冲MIG焊进行焊接，未补焊前共焊两道，保护气体为纯氩气体(99.995% Ar)，焊接工艺参数见表2所示.

表2　焊接工艺参数

Table 2　Welding process parameters

焊接顺序	焊丝直径 d/mm	焊接电流 I/A	电弧电压 U/V	焊接速度 v/(cm·min^{-1})	氩气流量 q/(L·min^{-1})
第一道	2.0	220~260	26~28	35~40	15~30
第二道	2.0	200~240	26~28	46~48	15~30
第三道	2.0	200~240	26~28	40~44	15~30

铝合金母材需在箱式电阻炉80~100 ℃的温度下预热15~20 min，坡口选择根据中华人民共和国国家标准GB/T 985.3—2008《铝及铝合金气体保护焊推荐坡口》.

采用GX-40金相显微镜以及JSM-6490LV型扫描电子显微镜观察母材及组织的显微形貌. 采用HV-10B进行硬度试验，试验载荷为100 N，载荷加

收稿日期: 2011-09-08
基金项目: 国家科技支撑计划资助项目(2009BAG12A04-D02)

载时间保持为10 s. 采用WDW3100万能材料试验机进行抗拉强度试验，试验过程中加载速度为1 mm/min. 采用JBN-300摆锤式冲击试验机进行冲击试验. 微型剪切试验采用自制设备，试验过程中预加载50 N，摩擦力30 N. 试验过程中，记录剪切最大力，并计算抗剪强度，然后，在位移-力曲线上找到断点，在断点处做位移的垂线与横轴相交. 微剪试样尺寸如表3所示.

表3 微剪试样尺寸(mm)

Table 3 Size for micro cutting test

焊接工艺	所取试件焊缝长度 l	横截面尺寸($a \times b$)
正常焊接	4.2	1.40×1.40
一次焊补	3.4	1.34×1.36
二次焊补	2.8	1.42×1.40
三次焊补	5.0	1.44×1.44

2 试验结果及分析

2.1 金相组织分析

图1～图4是各种焊接条件下金相微观组织形貌. 焊缝金相主要为α-相基体和其上分布着的部分析出的β-相. 经过焊接加热等强烈的反应，铸态化合物破碎，冷却后呈粒状均匀分布于基体上. 焊缝中心为树枝晶和等轴晶的混合. 在焊缝靠近熔合线一边，可以看到焊缝中存在方向性十分明显的柱状晶组织. 由于焊缝各部分的冷却速度不一，焊缝中心最后冷却，焊缝中部冷却较慢为等轴晶粒，晶粒均匀、细小，靠近母材的焊缝两边是垂直于熔合线的细长晶粒. 有些焊缝晶粒是在母材晶粒基础上长大的，因此也称之为半熔化区. 熔合区的组织变化很大，且各向异性，所以熔合线区对接头的性能影响很大，拉伸断裂常出现于此[5].

不同次数焊补金相组织中可以明显看到焊补层与未焊补焊缝组织的不同，焊补层的晶粒比原焊缝的大，α(Al)+β(Mg_2Al_3)共晶网状组织变得更大. 焊补层的融合区的受热析出的第二相也更多[6].

通过各次焊补的金相组织对比，焊补层和原焊缝的金相有明显界限，焊补过后的试件，由于多了一次热输入，导致焊缝中的第二相聚集[7]. 在腐蚀过后，第二相溶解，所以看到的黑色凹坑比正常焊接时候大. 铝合金焊接接头靠近焊缝边缘有一条很窄的熔合区，形成了细小的等轴晶组织，紧接着为完全再结晶组织及不完全再结晶组织.

焊缝中形成的气孔主要来源于熔池中的H元素，熔池中存在很多附着界面，如母材未熔化的固态晶粒、分布不均的溶质质点等，为氢气泡的非自发形核提供了必备条件. 随着焊补次数的增多，焊接熔池中存在的缺陷增多，造成焊缝中的气孔数量增多.

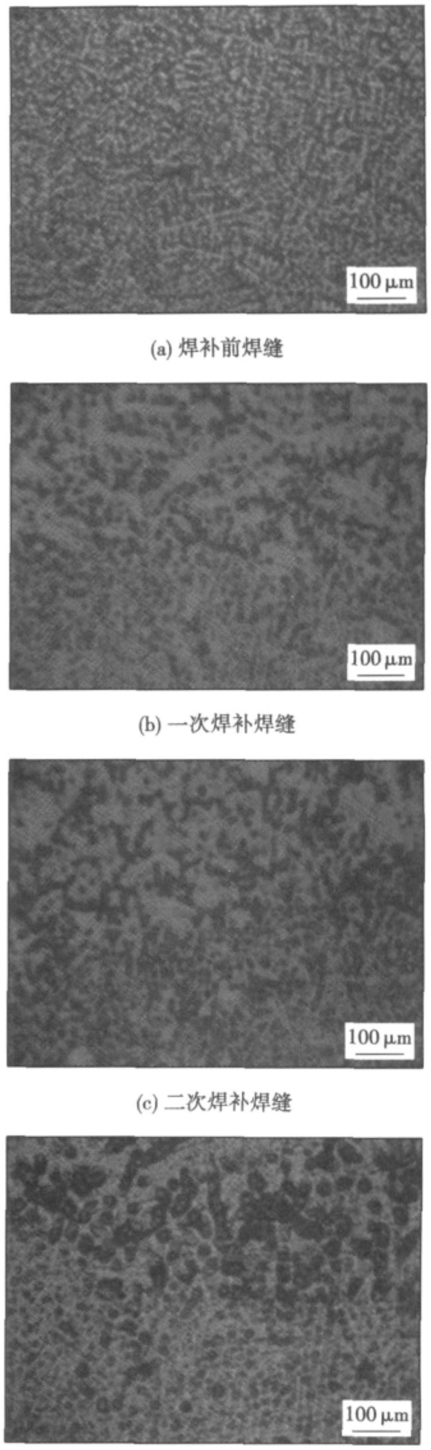

(a) 焊补前焊缝

(b) 一次焊补焊缝

(c) 二次焊补焊缝

(d) 三次焊补焊缝

图1 焊补前后焊缝显微组织

Fig. 1 Morphology of weld after and before welding

2.2 硬度试验结果及分析

图5是各种焊接条件下硬度的曲线对比. 焊缝硬度大大低于热影响区和母材，焊缝中心的硬度最

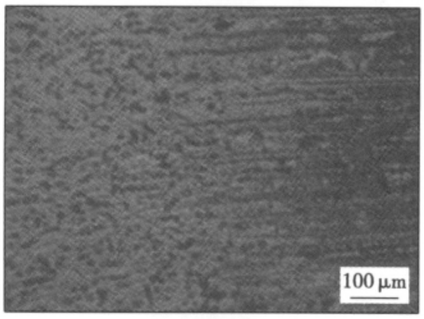

(a) 焊补前熔合区

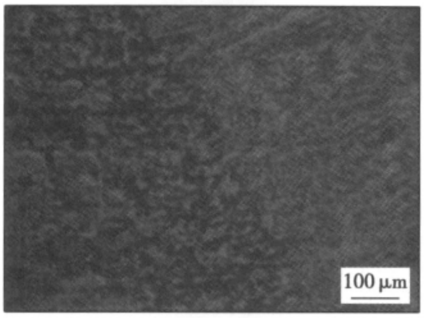

(b) 一次焊补熔合区

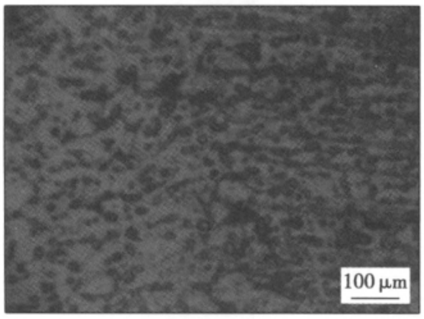

(c) 二次焊补熔合区

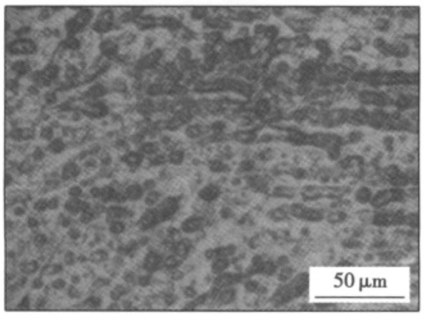

(d) 三次焊补熔合区

图 2　焊补前后熔合区显微组织

Fig. 2　Morphology of fusion zone after and before welding

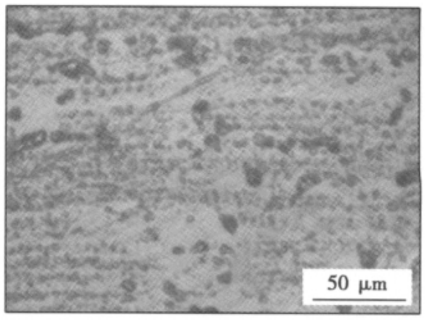

(a) 焊补前热影响区

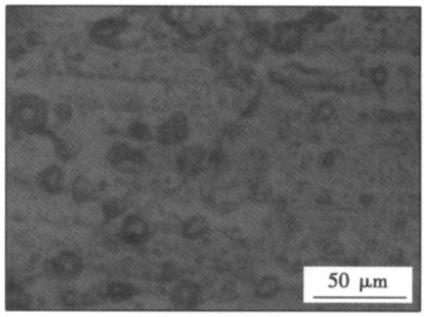

(b) 一次焊补热影响区

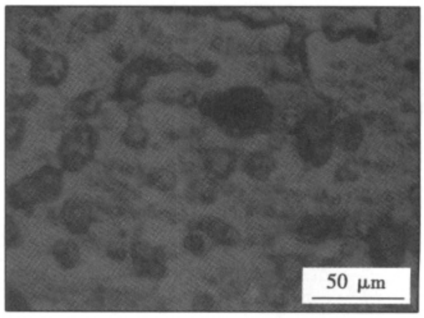

(c) 二次焊补热影响区

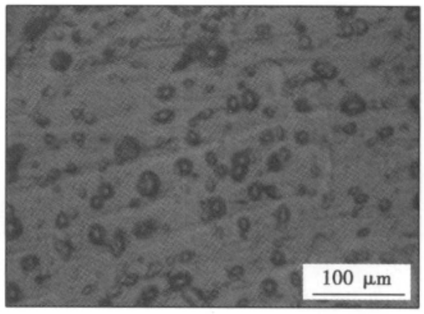

(d) 三次焊补热影响区

图 3　焊补前后热影响区显微组织

Fig. 3　Morphology of heat affected zone after and before welding

低，距离焊缝中心越远，硬度值越高. 焊补后接头的热影响区硬度高于未焊补接头的接热影响区. 熔合线附近区域的硬度梯度最大，性能发生突变，说明在熔合线附近性能很不均匀，加载时容易发生失稳[8].

2.3　拉伸试验结果及分析

图 6 是各种焊接条件下的接头抗拉强度. 一次焊补和二次焊补的接头抗拉强度平均值要略大于未焊补的接头，三次焊补的接头抗拉强度平均值要小于未焊补的接头.

5083 铝合金母材的抗拉强度为 290 MPa，焊接接头的抗拉强度均小于母材的抗拉强度，约为母材的 40%. 试验发现焊接接头拉伸断口部位都位于焊

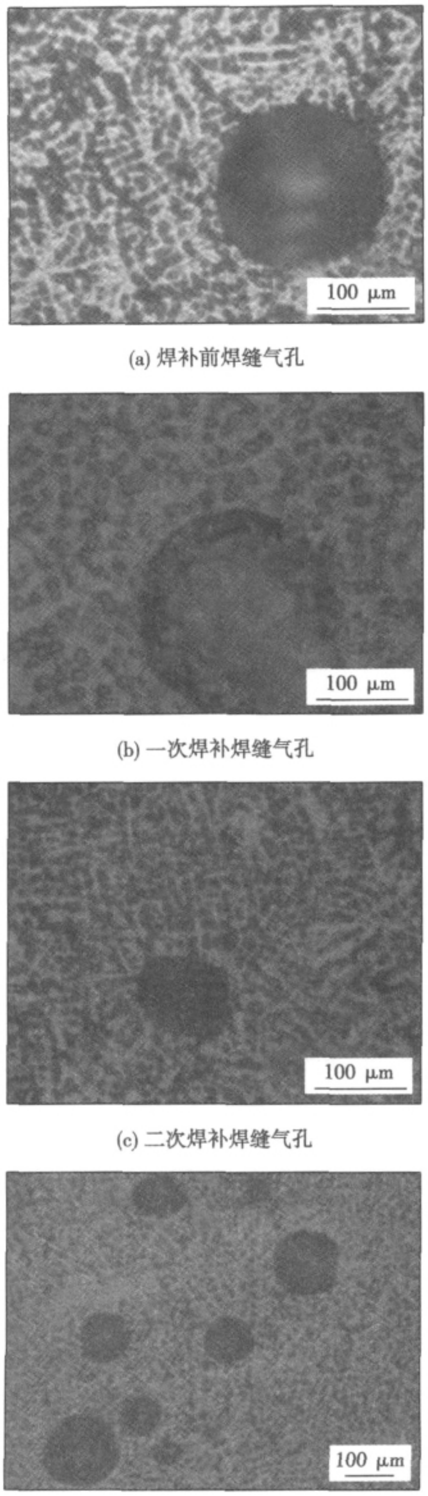

(a) 焊补前焊缝气孔

(b) 一次焊补焊缝气孔

(c) 二次焊补焊缝气孔

(d) 三次焊补焊缝气孔

图4 焊补前后气孔显微组织

Fig. 4 Morphology of pore after and before welding

缝. 断裂面与拉应力的方向大约呈现45°,断裂面总是从一个熔合线到另一个熔合线,剪切唇和放射区很明显,纤维区不明显. 同时可以发现断口中存在各类焊接缺陷,如气孔、夹渣等,这些缺陷的存在会降低接头的力学性能. 一次焊补与二次焊补及三次焊补之间的抗拉强度变化不大,说明在控制好工艺

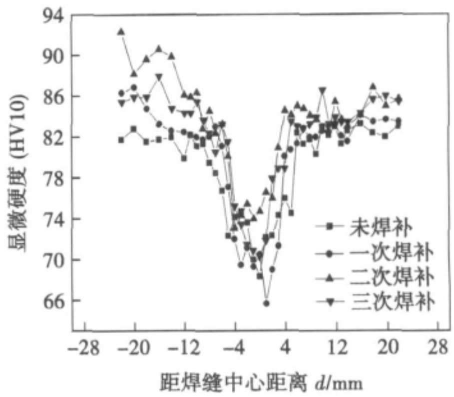

图5 多次焊补硬度对比

Fig. 5 Hardness test result for different times welding

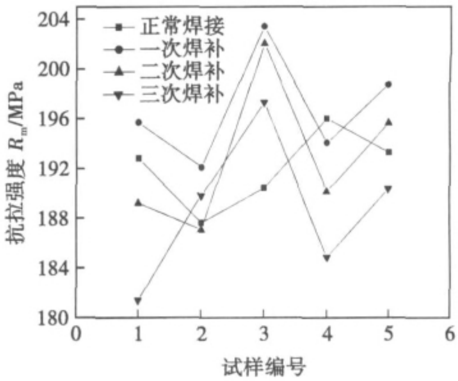

图6 多次焊补接头抗拉强度

Fig. 6 Tensile strength result for different times welding

和减少焊接缺陷的情况下,试件有进行三次焊补的可能.

2.4 冲击试验结果及分析

图7是各种焊接条件下接头冲击吸收功. 各个焊接接头的断口剪切唇区很明显,说明都是韧性断裂. 纤维区和放射区的面积有明显变化,随着焊补次数的增多,放射区的面积增大,而纤维区的面积减

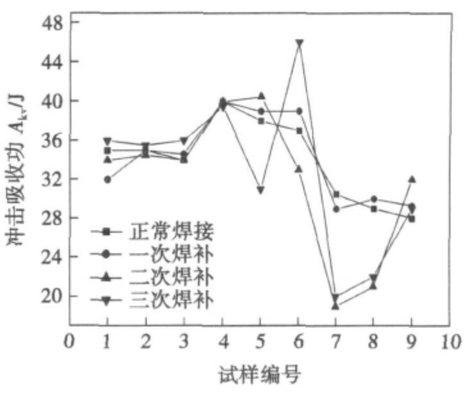

图7 多次焊接头的冲击吸收功

Fig. 7 Impact shock test result for different times welding

少，说明焊接接头变脆，这和上面的冲击功试验结果也是相符合的．由于母材离焊缝较远，焊接时温度较低，没有发生组织变化，所以不同次数焊补断裂缺口无变化，性能没有发生明显变化[9]．

2.5　冲击断口扫描电镜分析

从图 8 ~ 图 9 可以明显的观察到不管是焊缝还是热影响区的断口形貌大部分成韧窝状，并且等轴韧窝居多，这说明断裂性质是韧性断裂．并且还可

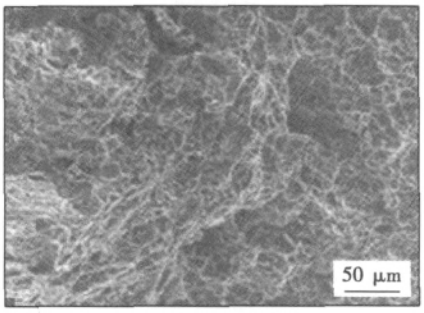

(a) 焊补前焊缝

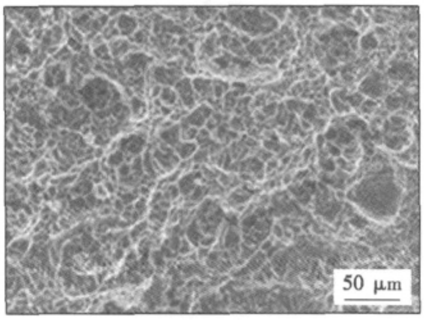

(b) 一次焊补焊缝

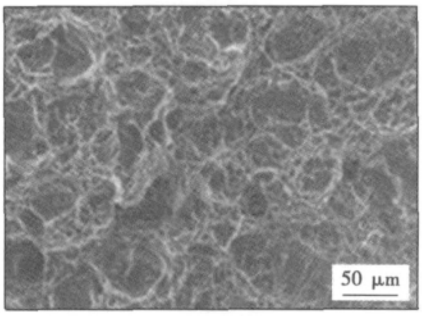

(c) 二次焊补焊缝

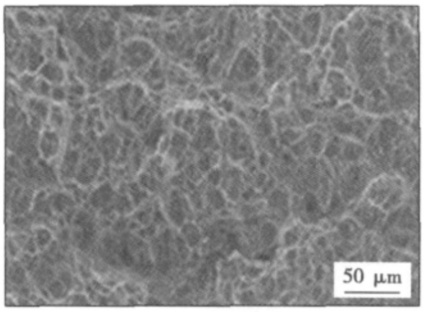

(d) 三次焊补焊缝

图 8　不同补焊次数焊缝冲击断口的显微组织形貌
Fig. 8　Morphology of weld after impact shock test

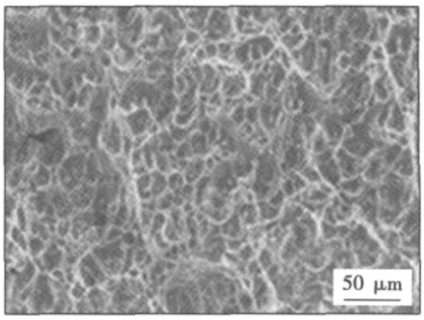

(a) 焊补前热影响区

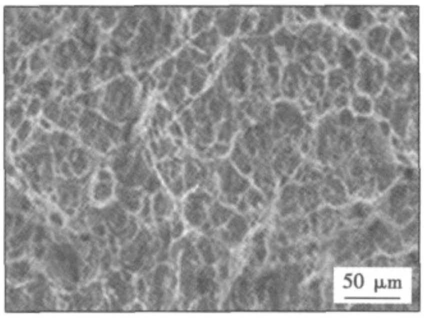

(b) 一次焊补热影响区

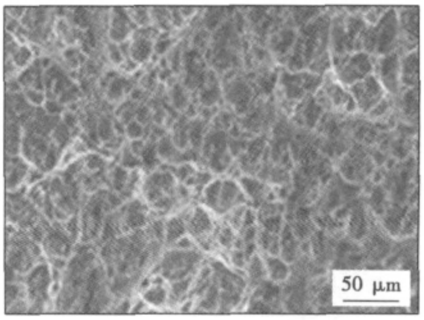

(c) 二次焊补热影响区

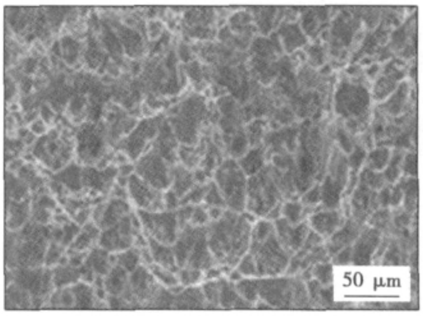

(d) 三次焊补热影响区

图 9　不同补焊次数热影响区冲击断口的显微组织形貌
Fig. 9　Morphology of heat affected zone after impact shock test

以从图 8 明显看出韧窝随着焊补次数的增多而增大，说明材料随着焊补次数的增多韧性下降．从图 9 可以发现随着焊补次数增多热影响区断口形貌基本没多大变化，仍为等轴韧窝．

2.6　微型剪切试验结果及分析

图 10 是不同焊补次数接头抗剪强度分布曲线．

焊缝处抗剪强度比较低，试件有一定的软化区，但是软化区不明显，热影响区宽度大约 10 mm，可以发现经过焊补的试件整体低于未焊补的试件，但是下降得不多，并且不同焊补次数接头之间的抗剪强度差别并不大，说明试件经过焊补，抗剪切能力下降，但是趋于稳定，三次焊补质量几乎和二次焊补一样.

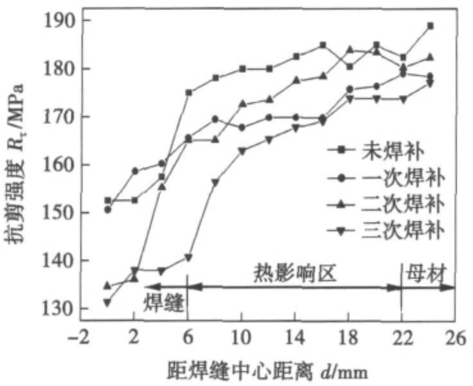

图 10 不同焊补次数接头抗剪强度

Fig. 10 Strength curves of micro cutting after welding

图 11 是不同焊补次数接头压入率分布曲线. 焊接接头焊缝区的压入率最大，说明焊缝区的塑性最好. 而热影响区的压入率降低，说明其塑性降低，这是由于热影响区再结晶，导致晶粒细化的结果.

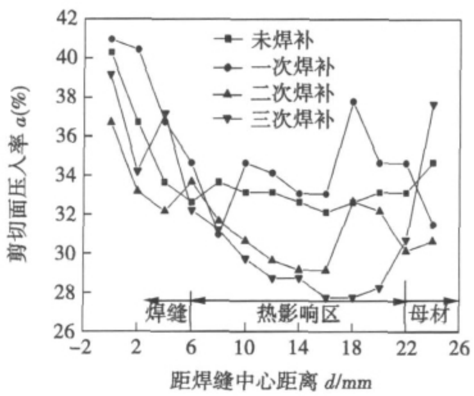

图 11 不同焊补次数接头压入率分布曲线

Fig. 11 Push rate curves of micro cutting after different times welding

3 结 论

(1) 5083 铝合金各次焊补的焊缝及热影响区的硬度均低于母材的硬度，热影响区产生了软化. 5083 铝合金焊补后热影响区硬度比未焊补热影响区硬度略高. 铝合金焊接接头焊缝区为铸态组织. 由于焊缝金属为熔化的 ER5356 铝镁焊丝所填充，因此焊缝金属的硬度较低.

(2) 焊缝处抗剪强度比较低，焊补后，抗剪切能力下降，但是趋于稳定.

(3) 三次焊补与二次焊补比较，性能并没有明显差异，所以有进行三次焊补的可能.

参考文献:

[1] 路 浩，马子奇，刘雪松，等. 300 Km/h 高速列车车体残余应力超声波法无损测量[J]. 焊接学报，2010，31(8)：29-31.
Lu Hao，Ma Ziqi，Liu Xuesong，*et al*. Ultrasonic residual stress measurement of 300 km /h high speed train body[J]. Transactions of the China Welding Institution，2010，31(8)：29-31.

[2] 陆善平，魏世同，李殿中，等. 焊丝成分对高速列车转向架焊接接头性能的影响[J]. 焊接学报，2010，31(6)：21-24.
Lu Shanping，Wei Shitong，Li Dianzhong，*et al*. Effects of welding w ire composition on properties of welding joints for high speed train bogie[J]. Transactions of the China Welding Institution，2010，31(6)：21-24.

[3] 苟国庆，黄 楠，陈 辉，等. 高速列车 A7N01S-T5 铝合金焊接接头盐雾腐蚀行为分析[J]. 焊接学报，2011，32(10)：17-20.
Gou Guoqing，Huang Nan，Chen Hui，*et al*. Analysis on corrosion behavior of welded joint of A6N01-T5 aluminum alloy for high-speed train[J]. Transactions of the China Welding Institution，2011，32(10)：17-20.

[4] 满伯倩，胡明华，卢碧琨. 2A14 铝合金返修焊技术[J]. 上海航天，2005(3)：61-64.
Man Boqing，Hu Minghua，Lu Bikun. Rewelding of 2A14 aluminum alloy[J]. Aerospace Shanghai，2005，(3)：61-64.

[5] 谢志勇，杨晖虹. 焊接接头特性对铝合金在机车车辆上应用的影响[J]. 电力机车与城轨车辆，2004，27(5)：46-47.
Xie Zhiyong，Yang Huihong. Effect of welded joint performance on aluminum alloy applying in railway vehicles[J]. Electric Locomotives &Mass Transit Vehicles，2004，27(5)：46-47.

[6] Olaf E. 铁路车辆的铝焊接结构件[J]. 国外机车车辆工艺，1992(4)：12-19.
Olaf E. Aluminum weldingweldments of railway vehicles[J]. Locomotive & Rolling Stock Technology，1992(4)：12-19.

[7] 贺运嘉. 金属材料熔焊工艺[M]. 西安：西北工业大学出版社，1980.

[8] 周振丰，张文钱. 焊接冶金与金属焊接性[M]. 北京：机械工业出版社，1988.

[9] Lawrence F V，Munse W H. Effects of porosity on tensile properties of 5083 and 6061 aluminum alloys weldments[J]. Welding Res Counc Bull，1999，22(7)：326-334.

作者简介: 于金朋，男，1979 年出生，博士研究生，工程师. 主要从事高速列车车体结构研发设计工作. 发表论文 10 余篇. Email：jxsj01330@163.com

通讯作者: 张立民，男，博士，研究员. Email：zhang-lm01@163.com

boundaries weakened. Impact toughness of the weld metal is not improved due to the boundaries of δ-ferrite are apt to become the crack sources when the weld metal is subjected to impact loads. Meanwhile, superior impact toughness is obtained by normalizing and tempering heat treatment for δ-ferrite is eliminated after the treatment and the weld metal of the joint transforms to tempered martensite which is the same to the base metal.

Key words: China low activation martensitic steel; vacuum electron beam welding; microstructure; impact toughness

Welded joint strength and analysis for HAZ softening behavior of high Ti and Nb precipitation strengthened high strength steel DONG Xianchun, ZHANG Nan, CHEN Yanqing, ZHANG Xi, MU Shukun, ZHANG Feihu, SHENG Hai (Shougang Research Institute of Technology, Beijing 100043, China). pp 72-76

Abstract: Welded joint's tensile strength of high Ti and Nb precipitation strengthing high strength steel with MAG(80% Ar+20% CO_2) was tested. The results show that the welded joint strength decreases with the increasing of the heat input. The hardness of the HAZ is lower than the base metal, and the HAZ has softening behavior. The growth of the grain and dissolution of the (Ti, Nb, Mo)(C, N) second phase particle (<10 nm) in CGHAZ weakend the precipitation strengthing. The particle without dissolution hold C and Mo, which weaken the stability of the overcooling austenite. The CGHAZ can not have lath martensite or bainite with high hardness, but has granular bainite with low hardness. The decreasing of the precipitation strengthing can not be balanced by structure strengthening, which leads to softening behavior in CGHAZ. The coarsing of the (Ti, Nb, Mo)(C, N) second phase particle (<10 nm) in FGHAZ, which offsets the critical size with best precipitation strengthing, weakened the precipitation strengthing, led to softening behavior in FGHAZ.

Key words: precipitation strengthing; high strength steel; welded joint strengthing; HAZ softening behavior; second phase particle

Influence of several times welding reworking on aluminum alloy welding joints for high speed train YU Jinpeng[1,2], ZHANG Limin[1], ZHANG Weihua[1], CHEN Hui[1], MA Jijun[2] (1. Traction Power State Key Laboratory, Southwest Jiaotong University, Chengdu 610031, China; 2. CNR Tangshan Co., Ltd, Tangshan 063035, China). pp 77-82

Abstract: One time, second time and third time welding reworking test were employed to test the EN 5083 welding joints. The morphology, hardness, tensile strength, impact toughness, cutting strength and push rate were analyzed. The results showed that the grains of the reworking layers were larger than the original welding layers. The α(Al)+β(Mg_2Al_3) net like morphology were much larger. The second phase after heated of the fusion area was much more than the original welding layers. The hardness, tensile strength, impact toughness were the same as the original welding layers. The cutting tongue of fracture was obviously which manifested the fracture mechanism was toughness. The cutting strength of the weld was lower but distributed stable. The cutting strength of different layers was the same as original which manifested the properties of the welding reworking layers were well. So the third reworking may be possible.

Key words: EN 5083 aluminum alloy; several times welding reworking; second phase; toughness fracture

Effect of energy arrangement on temperature field and stress field in dual-beam laser welding process with filler wire LEI Zhenglong[1], CHEN Yanbin[1], LV Tao[1], DIAO Wangzhan[1], SUN Zhongshao[2], CHEN Jilun[2] (1. State Key Laboratory of Advanced Welding and Joining, Harbin Institute of Technology, Harbin 150001, China; 2. Capital Aerospace Machinery Company, Beijing 100076, China). pp 83-88

Abstract: The heat source model of double-cylinder heat source + surface heat source is established in dual-beam laser welding process. Based on the finite element software Marc, the temperature field and stress-strain field of dual-beam laser welding with filler wire are simulated when the distance between two beams is 0.6 mm. And the effect of energy arrangement on the temperature characteristics and residual stress distribution are analyzed. The simulated results show that the heat melting efficiency decreases gradually with the decrease of the angle between the beam and the weld center. The residual stress mainly concentrate on longitudinal tensile stress in weld zone. At the same time, it can be found that the energy arrangement mainly affect the residual stress distribution and the angular deformation of the weld, while the effect on the maximum residual stress is not obvious.

Key words: Dual-beam laser welding; energy arrangement; temperature field; residual stress; numerical simulation

Soft-switch DC chopper four fold-frequency power control 300 KHz/50 kW induction welding power SHEN Jinfei, ZHAO Hui, YANG Lei (College of Electrical Engineering, Jiangnan University, Wuxi 214122, China). pp 89-92

Abstract: A four times frequency IGBT 300KHz induction welding power is put forward. Power control is composed with three-phase diode bridge inverter and DC chopper circuit. The chopper circuit adopts active nondestructive buffer buck converter , and in a wider range of the load the main, deputy switch tube and free-wheeling diode are achieve soft switch. The four groups of IGBT inverter in parallel are used for each IGBT in time-sharing control. The work frequency of the inverter is four times of the frequency IGBT switch. The inverter works in the load resonant state, and the switch tube works in shutting off at ZCS and switching on and off at ZVS. The output 300 kHz/50 kW serial-resonant inductive welding power was designed, and the design parameters and test waveforms were given. The results show that it is possible to produce capacity of high frequency induction heat welding power by using the method of four-times frequency control points with IGBT alternative power MOSFET.

Key words: induction welding; soft chopped; softswitch; fourfold frequency; time-sharing control

Effect of titanium on microstructure and properties of Zn-22Al filler metals YANG Jinlong[1], XUE Songbai[1], JI Feng[1], WANG Kebing[2], SUN Bo[2], Wang Shuiqing[2] (1. College of Materials Science and Technology, Nanjing University of Aero-